Science, Engineering and Technology Vol. 3, No. 1, pp. 44-49
www.setjournal.com *https://doi.org/10.54327/set2023/v3.i1.79*

Analytical and Numerical Contact Stress Analysis of Spur Gears

Blagoja Nestorovski, Petar Simonovski

Ss. Cyril and Methodius University in Skopje, Faculty of Mechanical Engineering, North Macedonia

Abstract

The damage that occurs on the teeth flank of cylindrical gears is a complex phenomenon and depends on many factors. The most common cause for these damages is the high contact stress of the meshing gears. Although this contact pressure, by itself, cannot be a criterion for determining the durability of the gears, a good correlation has been found between the contact or Hertz pressure and the damage that occurs on the tooth flank. This paper analyzes the influence of the pressure angle α on the contact stress. Analytical calculation according to the ISO 6336-2:2006 and finite element method (FEM) was used for the analysis. Four cases were analyzed with a change in the pressure angle, i.e., cylindrical spur gears and pressure angles of 17.5°, 20°, 22.5° and 25°. In the results, it was noted that by increasing the pressure angle, the contact stress decreases. It can also be concluded that by increasing the pressure angle, the difference in the results between the analytical and FEM analysis, also increases.

Keywords: *Hertz pressure, contact stress, pitting, spur gear, FEM*

1. Introduction

Due to the advantages of gears, such as a constant transmission ratio, long service life, and high load capacity, gears are one of the most used machine elements for mechanical power transmission. There are many types of gears, but some of the most used are spur and helical gears. The main difference between these gears is that the teeth of the spur gears are parallel to the axis of rotation, and in helical gears, they are inclined by an angle β with respect to the axis of rotation. Helical gears, compared to spur gears, have a higher load capacity, but also quieter operation due to reduced vibrations. The contact between the teeth in the spur gears begins simultaneously along the entire width of the gear. In helical gears, it starts at one point on the edge of the tooth and gradually continues along the entire width of the gear, thus contributing to the quieter operation of gears [1-3].

The contact conditions of the meshing gears continuously change, contributing to various defects occurring along the flank of the tooth [4]. Meshing gears are usually loaded with two types of stress: bending stress and surface stress caused by the contact of the teeth. In the case of high contact stress, damage occurs on the side of the tooth, which is called pitting [5].

Pitting is one of the most common failures [6] that occurs in gears and represents fatigue due to the repetition of high contact stress. This damage occurs when the contact stress exceeds the surface fatigue strength. The contact stress is directly related to the loading condition of the gear, as well as to the geometrical characteristics of the gear and gear material. The authors in [7] analyzed the influence of the gear module on the contact stress using the finite element method (FEM), and the results were compared with those from Hertz's equation. The results show that by increasing the module, the maximum contact stress decreases. In [8], the contact stress of spur gears under different loading conditions was analyzed using ANSYS Workbench. The results were compared with those from theoretical calculations, which showed a difference of less than 10% between them. The influence of the static friction coefficient on the contact stress in meshing spur gears was analyzed in [9]. Using the FEM,

Corresponding author: *Blagoja Nestorovski (blagoja.nestorovski@mf.edu.mk)*
Received*: 4 April 2023;* Revised: *11 April 2023;* Accepted*: 24 April 2023;* Published*: 25 April 2023*

it was concluded that the contact stress increases with an increase in the value of the friction coefficient. Contact stress analysis using different materials was conducted in [10].

Although gears with a pressure angle of 20° are preferred, the angle changes under certain situations. Increasing the pressure angle improves the gear strength, but also increases noise during the operation of the gears. Reducing the pressure angle reduces the load-carrying capacity of the gears but also results in quieter operation. This study aimed to determine the effect of changing the pressure angle on the contact pressure. Analytical methods and FEM were used to determine the change in contact stress. Four cases were analyzed with pressure angles of 17.5°, 20°, 22.5°, and 25°. The gear loading conditions, materials, and other geometrical characteristics remained the same for all four cases.

2. Gear Contact Stress Calculation

Tooth flank damage, or pitting, in spur gears due to fatigue from repetitive gear loads is a complex problem. This damage occurs in the form of pits on the tooth flank (Figure 1). The most common reason for this is the high contact pressure, which exceeds the permissible limit.

Figure 1. Graphical illustration of gear pitting.

The maximum contact pressure can be calculated according to the Hertzian theory, which is based on the contact between two cylinders. Hertz's theory assumes that the pressure distribution in the contact area is elliptical (Figure 2) [11, 12]. This theory can also be applied to involute gears because of the involute shape of the tooth flank.

Although the maximum contact pressure cannot be considered as a criterion for pitting occurrence, a good correlation was found between the maximum contact pressure and pitting. As a result, the Hertz pressure or Hertz stress is often used as a basis for surface durability calculations [5].

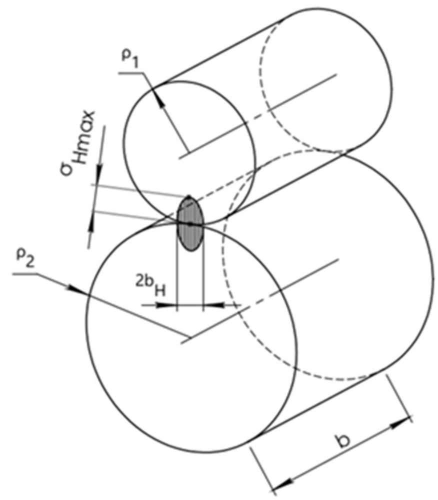

Figure 2. Hertz contact theory [5, 7].

According to ISO 6336-2:2006, the formula for calculating the nominal contact stress at pitch point P (Figure 3), for flawless gearing (ideal gears without errors, meaning that application and dynamic factors are not included in the calculation), and because of the application of constant nominal torque, is as follows [5]:

$$\sigma_{H0} = Z_H Z_E Z_\varepsilon Z_\beta \sqrt{\frac{F_t}{bd_1} \frac{u+1}{u}} \qquad (1)$$

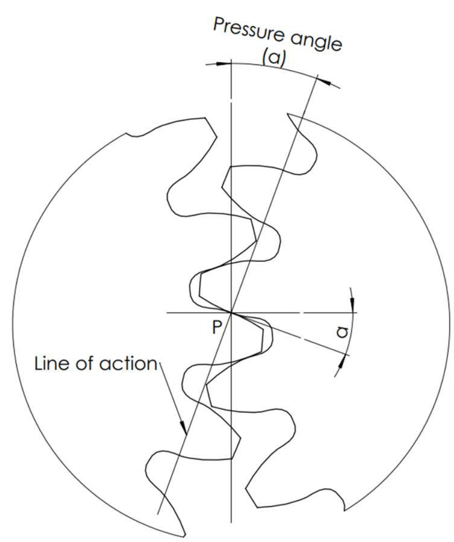

Figure 3. Pressure angle α.

Table 1. Specification of gear set.

Parameter	Case A		Case B		Case C		Case D	
	Pinion	Gear	Pinion	Gear	Pinion	Gear	Pinion	Gear
Number of teeth	20	20	20	20	20	20	20	20
Module [mm]	4	4	4	4	4	4	4	4
Pressure angle [°]	17.5	17.5	20	20	22.5	22.5	25	25
Pitch Diameter [mm]	80	80	80	80	80	80	80	80
Face Width [mm]	20	20	20	20	20	20	20	20
Material Young's modulus [N/mm^2]	206 000							
Poisson's ratio	0.3							
Torque [Nm]	300							
Contact force [N]	7500							

The *zone factor* Z_H for spur gears can be calculated according to the following relationship:

$$Z_H = \sqrt{\frac{2}{sin\alpha \cdot cos\alpha}} \qquad (2)$$

where,

α- Normal pressure angle.

The *elasticity factor* Z_E depends on the reduced modulus of elasticity E_r and can be calculated using the following equation:

$$Z_E = \sqrt{\frac{E_r}{2\pi}} = \sqrt{\frac{1}{\pi(\frac{1-v_1^2}{E_1}+\frac{1-v_2^2}{E_2})}} \qquad (3)$$

where,

E_1, E_2- Material Young's modulus, for pinion and gear, respectively,

v_1^2, v_2^2- Poisson's ratio, for pinion and gear, respectively.

When $E_1 = E_2 = E$, and $v_1 = v_2 = v$, and for $v = 0.3$ (for steel and aluminum), the equation becomes:

$$Z_E = \sqrt{0.175E}.$$

The *contact ratio factor* Z_ε can be calculated using the following equation:

$$Z_\varepsilon = \sqrt{\frac{4-\varepsilon_\alpha}{3}\left(1-\varepsilon_\beta\right)+\frac{\varepsilon_\beta}{\varepsilon_\alpha}} \qquad (4)$$

where,

ε_α- Transverse contact ratio,
ε_β- Overlap ratio,

For spur gears, the overlap ratio ε_β=0.

The *helix angle factor* Z_β can be calculated according to the equation:

$$Z_\beta = \frac{1}{\sqrt{cos\beta}} \qquad (5)$$

where,

β- Helix angle, for spur gears, or $\beta = 0$, the helix angle factor $Z_\beta = 1.$

F_t is *the nominal tangential force* and can be calculated using the following equation:

$$F_t = \frac{2T}{d_1} \qquad (6)$$

where,

T- Nominal torque,
d_1- Pitch diameter.

The contact stresses for the cylindrical spur gears with pressure angles of 17.5°, 20°, 22.5°, and 25° were calculated using Equation (1), and the detailed specifications of the gear sets are listed in Table 1. In all four sets, only the pressure angle was changed; other specifications such as the number of teeth, module, material, face width, etc., were unchanged.

The nominal tangential force was calculated according to Equation (6) as follows:

$$F_t = \frac{2T}{d_1} = \frac{2 \cdot 300\,000}{80} = 7500\ N$$

The corresponding factors are calculated based on equations (2-5) and the pressure angle only influences the coefficients Z_H and Z_ε. The individual calculations for each case, are presented as follows:

- Case A, with a pressure angle of 17.5°

$$\sigma_{H0} = Z_H Z_E Z_\varepsilon Z_\beta \sqrt{\frac{F_t}{bd_1}\frac{u+1}{u}}$$
$$= 2.64 \cdot 189.8 \cdot 0.89 \cdot 1$$
$$\cdot \sqrt{\frac{7500}{20 \cdot 80}\frac{1+1}{1}} = 1365.45\ MPa$$

- Case B, with a pressure angle of 20°

$$\sigma_{H0} = Z_H Z_E Z_\varepsilon Z_\beta \sqrt{\frac{F_t}{bd_1}\frac{u+1}{u}}$$
$$= 2.49 \cdot 189.8 \cdot 0.90 \cdot 1$$
$$\cdot \sqrt{\frac{7500}{20 \cdot 80}\frac{1+1}{1}} = 1302,34\ MPa$$

- Case C, with a pressure angle of 22.5°

$$\sigma_{H0} = Z_H Z_E Z_\varepsilon Z_\beta \sqrt{\frac{F_t}{bd_1}\frac{u+1}{u}}$$
$$= 2.38 \cdot 189.8 \cdot 0.92 \cdot 1$$
$$\cdot \sqrt{\frac{7500}{20 \cdot 80}\frac{1+1}{1}} = 1272.47\ MPa$$

- Case D, with a pressure angle of 25°

$$\sigma_{H0} = Z_H Z_E Z_\varepsilon Z_\beta \sqrt{\frac{F_t}{bd_1}\frac{u+1}{u}} = 2.29 \cdot 189.8 \cdot 0.93 \cdot 1$$
$$\cdot \sqrt{\frac{7500}{20 \cdot 80}\frac{1+1}{1}} = 1237.66\ MPa$$

3. FEM of Meshing Gears

The involute spur gear 3D models for the four cases were prepared using the parametric modeling software SolidWorks. The detailed specifications of the gears' parameters are listed in Table 1. The 3D models were exported to the FEM analysis software, ANSYS Workbench.

The characteristics of the material used in the analysis is listed in Table 1. Frictionless contact was defined between the contact surfaces of the pinion and gear. The meshed model is shown in Figure 4. The ANSYS mesh control option was used to define the element size. As shown in Figure 4, a smaller element size is used around the contact zone between the pinion and the gear.

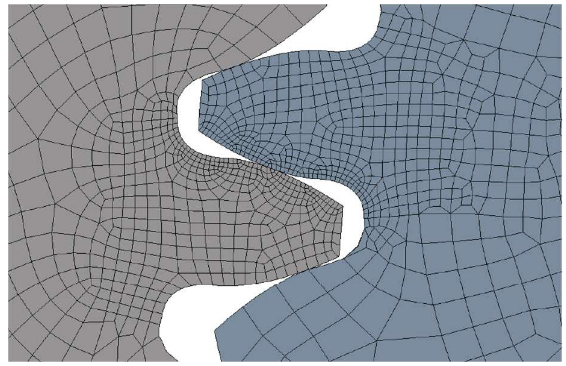

Figure 4. Meshed model of gear pair with pressure angle α=20°.

The boundary conditions are shown in Figure 5. A cylindrical support was defined on surfaces A and B (Figure 5). At reference point D, a moment of 300 Nm was applied, and at reference point C, remote displacement was defined. Remote displacement is a guided displacement of a part around a point. In this case, a rotation of 0.5° is defined around the reference point C, the directions of the remote displacement and moment are counterclockwise (Figure 5). It should be noted that the directions shown in Figure 5 do not refer to the direction of motion of the gears; they only refer to the setup in ANSYS Workbench, that is, at point D, the direction of the moment, and at point C, the direction of the remote displacement. In all four cases, mesh control and boundary conditions remain unchanged.

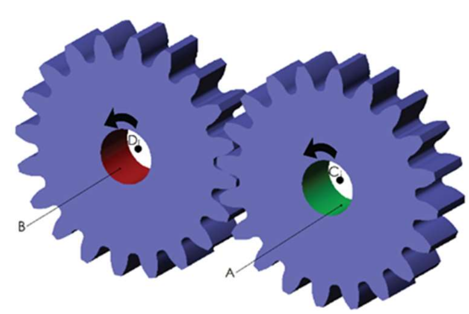

Figure 5. Boundary condition of FE model.

4. Results and Discussions

First, the contact stress for the four cases, that is, for pressure angles α of 17.5°, 20°, 22.5°, and 25°, was calculated using equation (1). Surface stress of 1365.45 MPa, 1302.34 MPa, 1272.47 MPa, and 1237.66 MPa were obtained, respectively. A finite element (FE) model was created, and the previously mentioned cases were analyzed. A graphical representation of the results of the analytical and FE analyses is shown in Figure 6 and the results of the analysis are shown in Figures 7-10. Based on these results, it can be concluded that as the pressure angle increases, the contact pressure decreases.

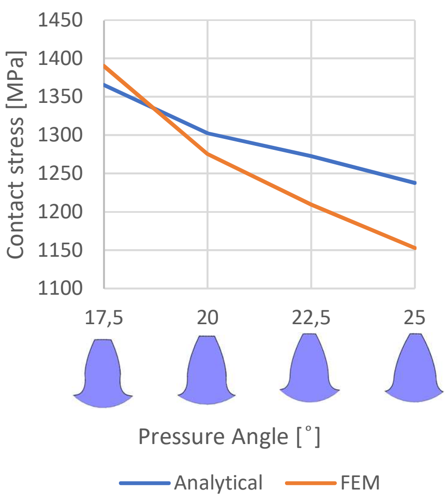

Figure 6. Graphical representation of the results.

A comparison was made between the results obtained using analytical calculations and those obtained using FEM. It was found that a larger difference between the results occurred at a larger pressure angle. The results are presented in Table 2.

Table 2. Difference between analytical and FEM results.

	Analytical [MPa]	FEM [MPa]	Difference [%]
Case A	1365.45	1390	1.8
Case B	1 302.34	1275.4	-2
Case C	1272.47	1209.5	-4.9
Case D	1237.66	1152.6	-6.8

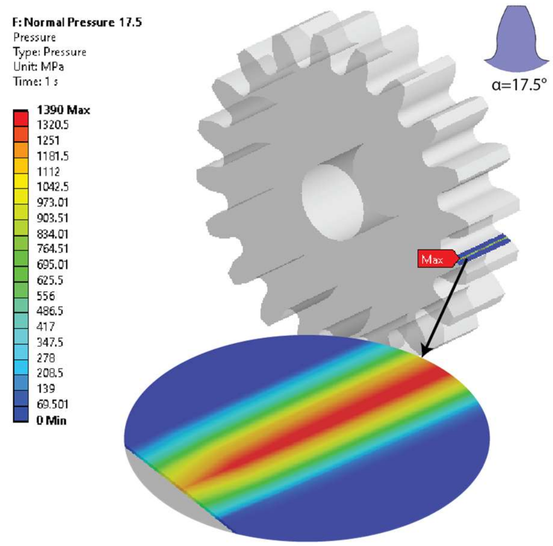

Figure 7. Maximum contact pressure from ANSYS Workbench for pressure angle α=17.5°.

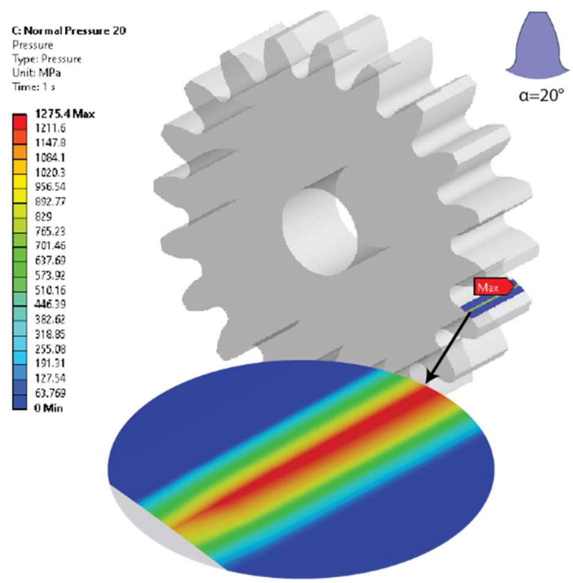

Figure 8. Maximum contact pressure from ANSYS Workbench for pressure angle α=20°.

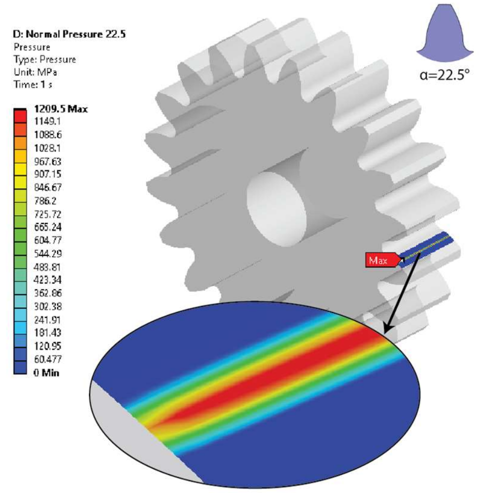

Figure 9. Maximum contact pressure from ANSYS Workbench for pressure angle α=22.5°.

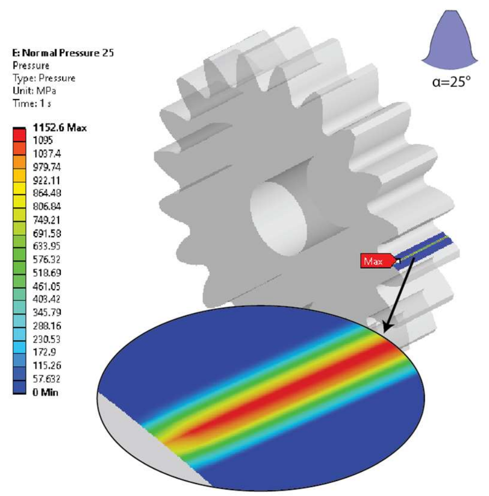

Figure 10. Maximum contact pressure from ANSYS Workbench for pressure angle α=25°.

5. Conclusion

When changing the pressure angle of meshing gears, all its effects on the load-carrying capacities of the gears should be considered. This study analyzed the influence of the pressure angle on the maximum contact pressure. From the results, it can be observed that by increasing the pressure angle, the maximum contact pressure decreases. The FE model was verified using analytical calculations and can be used in further research. This study analyzed only the maximum contact pressure but not the equivalent von Mises stress. Further research should be conducted on the impact of the change in the pressure angle on the equivalent stress.

Competing Interest Statement

The authors declare no known competing financial interests or personal relationships that could have influenced the work reported in this paper.

Data and Materials Accessibility

No additional data or materials were utilized for the research described in the article.

References

[1] M. Yaghoubi and H. Tavakoli, "Spur and Helical Gear Drives," *in Mechanical Design of Machine Elements by Graphical Methods*, Springer, Cham, 2022.

[2] X. Tang, L. Zou, W. Yang, Y. Huang, and H. Wang, "Novel mathematical modelling methods of comprehensive mesh stiffness for spur and helical gears," *Applied Mathematical Modelling*, vol. 64, pp. 524–540, 2018.

[3] V. I. Medvedev, A. E. Volkov, M. A. Volosova, and O. E. Zubelevich, "Mathematical model and algorithm for contact stress analysis of gears with multi-pair contact," *Mechanism and Machine Theory*, vol. 86, pp. 156–171, Apr. 2015.

[4] S. S. Patil, S. Karuppanan, I. Atanasovska, and A. A. Wahab, "Contact stress analysis of helical gear pairs, including frictional coefficients," *International Journal of Mechanical Sciences*, vol. 85, pp. 205–211, Aug. 2014.

[5] V. Vullo, "Surface Durability (Pitting) of Spur and Helical Gears," *in Gears, Springer Series in Solid and Structural Mechanics*, vol 11, Springer, Cham, 2020.

[6] X. Li, J. Li, C. Zhao, Y. Qu, and D. He, "Gear pitting fault diagnosis with mixed operating conditions based on adaptive 1D separable convolution with residual connection," *Mechanical Systems and Signal Processing*, vol. 142, p. 106740, Aug. 2020.

[7] B. Gupta, A. Choubey and G. V. Varde, "Contact stress analysis of spur gear," *International Journal of Engineering Research and Technology*, vol. 1, no. 4, pp. 1-7, Jun. 2012.

[8] C. Yao et al., "Finite Element Analysis of Dynamic Contact Stress of Spur Gear Based on ANSYS," *The Proceedings of the 9th Frontier Academic Forum of Electrical Engineering*, pp. 177–187, 2021.

[9] S. Patil, S. Karuppanan, I. Atanasovska, and A. A. Wahab, "Frictional Tooth Contact Analysis along Line of Action of a Spur Gear Using Finite Element Method," *Procedia Materials Science*, vol. 5, pp. 1801–1809, 2014.

[10] E. Eskezia and M. Abebaw, "Effect of Gear Materials on the Surface Contact Strength of Spur Gears," *Proceedings of Engineering and Technology Innovation*, vol. 22, pp. 50–59, May 2022.

[11] Y. Zhai et al., "Analysis of Tooth Surface Contact Stress of Involute Spur Gear," *Journal of Physics: Conference Series*, vol. 2133, no. 1, p. 012037, Nov. 2021.

[12] H. Loc and L. T. Anh, "Contact stress analysis and optimization of spur gears," *IOP Conference Series: Materials Science and Engineering*, vol. 1109, no. 1, p. 012004, Mar. 2021.